PHYSICAL REVIEW B VOLUME 46, NUMBER 8 15 AUGUST 1992-II

Anisotropic diffusion of hydrogen atoms on the Si(100)-2×1 surface

Christine J. Wu and Emily A. Carter
Department of Chemistry and Biochemistry, University of California, Los Angeles, California 90024-1569
(Received 14 February 1992)

This paper presents first-principles total-energy calculations of hydrogen-adatom diffusion on a Si(100)-2×1 reconstructed surface. The transition states for hydrogen-atom-diffusion pathways were established by mapping out the potential energy of a hydrogen atom jumping between the dangling bonds of a Si(100)-2×1 surface modeled by embedded finite silicon clusters. The diffusion barriers are high (2–3 eV) and wide (~3–4 Å), suggesting that H-atom diffusion on Si(100) proceeds via mostly a classical hopping mechanism instead of tunneling. Furthermore, diffusion of hydrogen atoms is predicted to be *anisotropic*, being preferentially directed parallel to the silicon-dimer rows, with an activation energy of 2.0 eV. Higher activation energies of 2.5 and 2.7 eV are predicted for diffusion perpendicular to dimer rows, for the cases of hydrogen atoms hopping from one dangling bond to a neighboring dangling bond on the same dimer and on an adjacent dimer, respectively. The mechanism for H-atom diffusion along dimer rows is markedly different from that previously proposed for Si-adatom diffusion on Si(100): H atoms are predicted to diffuse along edges of the dimer rows rather than down the middle.

I. INTRODUCTION

Diffusion of hydrogen atoms on silicon surfaces plays an important role in the kinetics of numerous chemical reactions of silicon with reagents containing hydrogen, e.g., Si_2H_6, (Ref. 1) H_2O, (Ref. 2) and NH_3.[3,4] In such reactions, hydrogen atoms are produced that migrate on the silicon surface until they eventually desorb to form gas-phase H_2 molecules. Indeed, the desorption of H_2 during chemical-vapor deposition on silicon is thought to be critical to further reaction, since it regenerates active sites for chemisorption, i.e., dangling bonds. As a result, understanding Si-H and H-H interactions in detail continues to be a subject of great interest. Hydrogen atoms are known to adsorb onto onefold sites of the Si(100)-2×1 surface, where they form strong Si-H bonds [3.3 eV (Ref. 5)–3.8 eV (Ref. 6)] to the dangling bonds on silicon dimers. In this coverage range ($\Theta_H \leq 1$ monolayer), the so-called monohydride phase is present, consisting of either zero, one, or two hydrogen atoms adsorbed on each surface Si dimer. Clearly, the structure of this phase, as well as subsequent desorption of H_2 gas, will be sensitive to the ability of H atoms to diffuse on the surface. Indeed, it is possible that adsorbate diffusion is the rate-limiting step in some desorption processes. It is still undetermined whether this is the case for H_2 desorption (β_1) form the monohydride phase of the Si(100)-2×1 surface, which recently has become the subject of some debate. Although it is agreed upon that β_1 H_2 desorption obeys first-order kinetics,[7–10] the desorption activation barriers reported by two groups measured by the same thermal-desorption technique differ by ~1 eV [2.0 eV (Refs. 7 and 8)–3.0 eV (Ref. 9)], while a recent measurement employing second-harmonic generation finds a barrier of 2.48±0.1 eV.[10] Consequently, very different β_1 desorption mechanisms have been proposed. Thus, an understanding of hydrogen-adatom diffusion on the Si(100)-2×1 surface and, in particular, a prediction of the hydrogen-diffusion activation energy may help to determine the β_1 H_2-desorption mechanism, especially for desorption at low hydrogen coverages where diffusion may indeed be rate limiting. In this paper, we focus on the determination of diffusion barriers for a single hydrogen atom on the Si(100)-2×1 surface by first-principles total-energy calculations and, at the same time, explore the underlying silicon-hydrogen interaction.

In contrast with the present work, previous studies of hydrogen diffusion on Si have examined only the (111) surface. Koehler *et al.*[11] studied hydrogen diffusion on Si(111)-7×7 using laser-induced thermal-desorption (LITD) techniques. They deduced an upper bound for the hydrogen-diffusion rate constant ($D \leq 10^{-9}$ cm^2/s) at 740 K, which indicates a low hydrogen mobility on Si(111)-7×7 even at relatively high temperatures. Reider *et al.*[12] conducted more quantitative measurements of hydrogen diffusion on Si(111)-7×7 by combining LITD with the second-harmonic-generation technique. They obtained a diffusion activation barrier of 1.5±0.2 eV and a preexponential factor $D_0 = 10^{-3}$ cm^2 s^{-1} over a temperature range of 670–730 K. Rice *et al.*[13] performed Monte Carlo simulations to study the diffusion of hydrogen atoms on a partially hydrogen-covered (H atoms covering all top sites) unreconstructed Si(111) surface using a semiempirical interaction potential, and predicted a classical diffusion activation barrier of ~2.6 eV, which is much higher than the experimental value.[12] However, since the structure of the Si(100)-2×1 surface bears almost no resemblance to the Si(111)-7×7 surface, we expect hydrogen-diffusion rates on Si(100)-2×1 to be distinctly different from those on Si(111)-7×7.

Detailed studies have also been carried out for hydrogen diffusion on metal surfaces.[14] On Ru(0001),[15–17] for example, a large hydrogen-diffusion coefficient ($D \sim 6.3\times10^{-4}$ cm^2/s at $T\sim260$–330 K) (Ref. 15) and a

 ©1992 The American Physical Society

low diffusion activation barrier (0.17±0.02 eV) are observed.[15] In contrast to its adsorption on silicon, hydrogen prefers to adsorb at a higher coordination site (threefold) on Ru(0001) with a smaller binding energy of ~2.9 eV.[18] Diffusion on semiconductors is expected to be radically different than diffusion on metals since adsorbate-surface bonds and bonds within the semiconductor surface involve directional covalent bonds rather than more delocalized metallic bonds. In general, adatom mobilities on metal surfaces are higher and more isotropic than those on semiconductor surfaces, which is consistent with the idea that the delocalized electron density of the metal allows the adatom to maintain a strong interaction with the surface throughout the diffusion event, while on Si, the localized dangling bonds simultaneously inhibit and control the direction of diffusion.

Several theoretical studies[19–22] have predicted Si self-diffusion on the Si(100)-2×1 surface to be anisotropic. Brocks *et al.*[19] reported activation energies of 0.6 and 1.0 eV for Si-adatom diffusion parallel and perpendicular to the dimer rows, respectively, using first-principles total-energy calculations within the local-density-functional approximation. Although they disagree with the classical simulation results using empirical potentials by Zhang *et al.*[20] and Srivastava *et al.*[21,22] about adsorption and diffusion sites, all of these investigations found anisotropic Si-adatom diffusion, with the preferred direction being along Si dimer rows.

In this paper, we present results of our studies of hydrogen self-diffusion on the Si(100)-2×1 surface, using first-principles total-energy calculations on embedded finite silicon clusters. The underlying hydrogen-silicon interaction potentials for diffusion both parallel and perpendicular to silicon dimer rows were mapped out. Saddle points for H-atom surface diffusion were obtained, yielding predictions of diffusion activation energies. The relative heights of these barriers suggest that anisotropic H-atom diffusion along Si dimer rows, similar but not identical to Si-adatom diffusion, occurs on the Si(100)-2×1 surface.

II. CALCULATIONAL DETAILS

The Si(100)-2×1 surface was modeled with the embedded finite Si clusters used in our previous work.[6,23,24] A key characteristic of the Si(100)-2×1 surface is the formation of silicon dimers in the $p(2\times1)$ reconstruction. Thus, all the clusters contained at least one Si surface dimer (the smallest repeat unit on the surface) and were embedded in modified H atoms ($\overline{\mathrm{H}}$ is used to represent inclusion of effects due to the rest of the Si lattice).[23–26] The $\overline{\mathrm{H}}$ atoms were represented by a minimum basis set of three Gaussian functions,[24] where the coefficients and exponents were optimized to mimic the electronegativity of a bulk Si atom, in order to avoid artificial charge transfer between Si and $\overline{\mathrm{H}}$ atoms. This effectively made all the subsurface Si atoms in the clusters bulklike, by allowing them to experience a tetrahedral, covalent environment. The core and valence electrons of the Si atoms were described by an effective core potential[27] and a valence double-ζ basis set, respectively, with d polarization functions ($\zeta^d=0.3247$) added only to the surface Si atoms. Chemisorbed H atoms were represented by the Dunning triple-ζ contraction[28] of the Huzinaga Gaussian basis set,[29] with one additional set of $2p$ polarization functions ($\zeta^p=0.6$). As an example, many of the calculations were performed using a $\mathrm{Si_9\overline{H}_{12}}$ cluster (shown below) that contains two surface Si atoms attached to four second-layer Si atoms, which in turn are connected to two third-layer Si atoms, and finally these third-layer Si atoms are bonded to one Si atom on the fourth layer. All subsurface Si atoms in this cluster have dangling bonds that are saturated by $\overline{\mathrm{H}}$ atoms to achieve a bulklike environment.

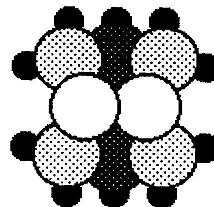

Our previous calculations on the $\mathrm{Si_9\overline{H}_{12}}$ cluster predicted the geometry of the Si(100)-2×1 surface[24] at the generalized valence bond with perfect-pairing restrictions[30] (GVB-PP) level using analytic gradient methods.[31,32]

For an accurate prediction of hydrogen-diffusion energetics, the inclusion of electron correlation is essential. However, performing high-level configuration-interaction (CI) calculations on the $\mathrm{Si_9\overline{H}_{12}}$ cluster is not computationally feasible at present. Therefore, we have developed a so-called geometry-mapping[6,24] (GM) procedure to construct a smaller GM-$\mathrm{Si_2\overline{H}_4}$ cluster, where the geometry of the top layers of the optimized $\mathrm{Si_9\overline{H}_{12}}$ cluster is mapped onto the GM-$\mathrm{Si_2\overline{H}_4}$ cluster. Thus, high-level CI calculations were carried out to calculate transition-state energies for two-dimensional hydrogen-diffusion pathways using the smaller GM clusters $[(\mathrm{Si_2\overline{H}_4})_{x=1,2}]$. Although in our earlier calculations[6] of the hydrogen-adsorption energetics on Si(100)-2×1 it was shown that the error caused by this geometry-mapping process (a cluster-size effect) is only ~0.1 eV, the cluster-size effect was reestimated in this work, since transition-state energies (barrier heights) may incur a different magnitude of error than binding energies (well depths). The details of this effect are discussed later.

The underlying Si-H interaction, which controls the self-diffusion of a single H adatom, was mapped out by solving for GVB, CI, and more general multiconfiguration self-consistent-field (MCSCF) wave functions and energies. In the GVB-PP calculations, the Si-dimer σ bonds and the Si-H bonds are correlated as GVB pairs (two orbitals per correlated pair of electrons). All CI expansions are generated from the restricted CI (RCI) multireference space, which contains direct products of all three possible configurations within each GVB pair. Calculations performed at the so-called GVB-CI level allow full variational freedom (a full CI) within an active space defined by the process, using the GVB-PP orbitals as a basis for the CI. In addition, GVB-CI-SCF calculations allow the orbitals of the GVB-CI wave func-

tion to be optimized simultaneously with optimization of the CI coefficients. Correlation-consistent CI (Refs. 33 and 34) (CCCI) calculations include more extensive electron correlation and yield more accurate predictions of energetics, because they allow full correlation to the entire CI basis of each electron pair involved in the process of interest. This method is nearly size consistent and was designed previously to achieve accurate predictions of bond-dissociation energies with a relatively small CI expansion.[33–36] In this paper, we extend the CCCI method further to calculate transition-state energies, which often involve more than one dominant configuration (resonance structure). We use the MCSCF wave function instead of the GVB-PP wave function as a starting point in the CCCI calculation, since the MCSCF wave function includes each of the resonance configurations involved in the transition state. Finally, even larger CI expansions $[SDT(3)+S_{val}]$ were performed for a H atom migrating from one onefold site to another on the same dimer. These $SDT(3)+S_{val}$ calculations included all single, double, and triple excitations to all valence orbitals from the three electrons involved in the diffusion path (i.e., the H atom and Si dangling-bond electrons) and all single excitations from all valence orbitals (which, by Brillouin's theorem, allows all the valence-orbital shapes to be optimized along the diffusion path). The reference space for these excitations was a direct product of a RCI in the Si-Si dimer bond and a GVB-CI within the H-atom and dangling-bond orbitals.

Our model for H-atom diffusion on Si(100)-2×1 is that H atoms adsorbed at onefold sites jump from one onefold site to another on the surface (localized hopping). We examined diffusion in the two principal directions, namely perpendicular to and along the Si-dimer row (shown in Fig. 1). Diffusion perpendicular to Si-dimer rows involves hydrogen (a) hopping from one dangling bond to another on the same Si dimer [shown in Fig. 2(a)], which was modeled by the GM-$Si_2\bar{H}_4H$ cluster, and (b) hopping from one dangling bond to another dangling bond on an adjacent Si dimer in an adjacent dimer row modeled by the GM-$Si_4\bar{H}_8H$(A) cluster [shown in Fig. 2(b)]. Diffusion along dimer rows involves H atoms hopping from one dangling bond to a dangling bond on an adjacent Si dimer in the same dimer row, which is modeled by the GM-$Si_4\bar{H}_8H$(S) cluster [shown in Fig. 2(c)]. (A) and

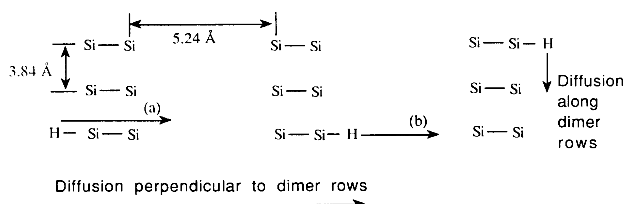

FIG. 1. Top view of hydrogen diffusion on the Si(100)-2×1 surface along two principal directions: (1) perpendicular to dimer rows, where hydrogen hops from one dangling bond to another either (a) on the same dimer or (b) on an adjacent dimer, and (2) along dimer rows, where hydrogen hops again from one dangling bond to another.

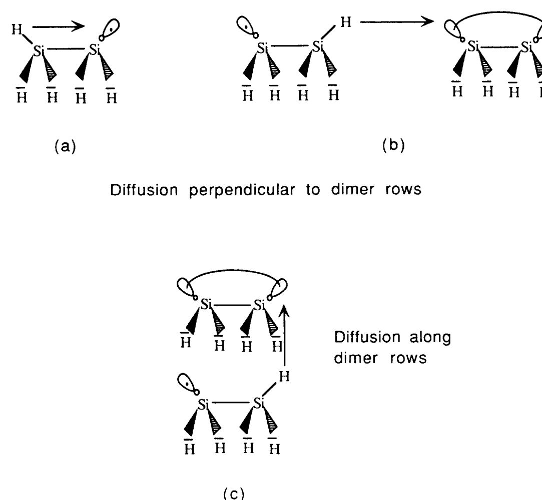

FIG. 2. Schematic structure of the GM clusters used to model hydrogen hopping from one dangling bond to another (a) on the same Si dimer, (b) on an adjacent Si dimer in an adjacent dimer row, and (c) on an adjacent Si dimer in the same dimer row. Equilibrium geometry of the onefold-coordinated H-Si-Si: θ_e(H-Si-Si)=114.0°, R_e(Si-H)=1.51 Å, R_e(Si-Si)=2.44 Å (see Ref. 6).

(S) are symbols that distinguish $Si_4\bar{H}_8H$ clusters representing dimers in adjacent dimer rows from those in the same dimer row.

In all calculations, the clusters are kept rigid when the H atom hops between dangling bonds and hence we are ignoring lattice motion during diffusion. Since the dangling bonds of Si dimers are very weakly coupled,[6] relaxation of the lattice during hydrogen surface diffusion is probably very small. Evidence for this comes from our previous work, which showed the Si-Si bond length of a H-Si-Si species is only 0.09 Å larger than that of the bare Si dimer.[6]

III. RESULTS AND DISCUSSION

In our model, hydrogen migrates from a particular onefold site to a neighboring onefold site via a twofold site, where it forms a bridging bond with the two dangling-bond orbitals of the surface Si atoms between which the H atom is hopping. Potential-energy curves were generated at the GVB-CI level for the three pathways discussed above, where H moves from one onefold site to another, while keeping the vertical distance to the surface fixed at that of the equilibrium geometry for the monohydride phase ($R_{\perp,e}$=1.373 Å).[6] The results are plotted in Figs. 3(a)–3(c) as a function of the distance parallel to the surface ($R_{\parallel}$), where $R_{\parallel}=0$ for H in the twofold bridging transition-state site and $R_{\parallel}=\pm1.85$ Å at the equilibrium Si-H distance. We see that the barriers are both high (~3 eV) and wide (~4 Å), which suggests that diffusion will occur only at high temperatures (as observed experimentally) and will proceed via a classical hopping rather than a tunneling mechanism.

We then relaxed the constraint of keeping the vertical distance fixed along the diffusion path, an approximation

that clearly leads to upper bounds on the true barrier heights. We did this by locating potential-energy minima ($E_\perp$) as a function of perpendicular distance ($R_\perp$) between the H atom and the surface dimer, while keeping the H atom at the twofold bridging position ($R_\parallel = 0$ at the transition state is imposed by the symmetry of the diffusion pathway). $E_\perp$ curves at the three hydrogen-diffusion transition states were calculated at the GVB-CI level and are plotted as a function of $R_\perp$ in Figs. 4(a)–4(c), respectively. From the minima in the $E_\perp$ curves, the equilibrium perpendicular distances between the H atom and the Si surface at the twofold bridging po-

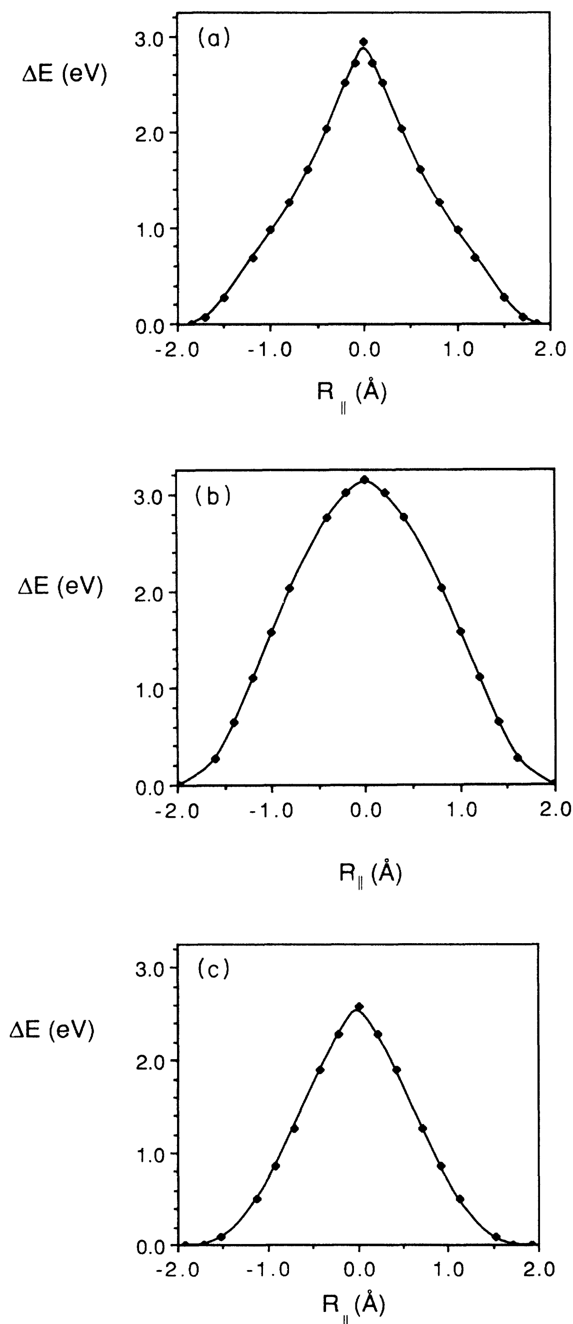

FIG. 3. GVB-CI potential-energy curves as a function of the H-atom distance measured parallel to the Si dimer from the midpoint of the dimer bond ($R_\parallel$), for H moving across from a onefold site to another (a) on the same dimer, (b) on an adjacent dimer in an adjacent dimer row, and (c) on an adjacent dimer in the same dimer row, while keeping the perpendicular distance fixed at that of the equilibrium onefold site ($R_{\perp,e}^{1F} = 1.373$ Å).

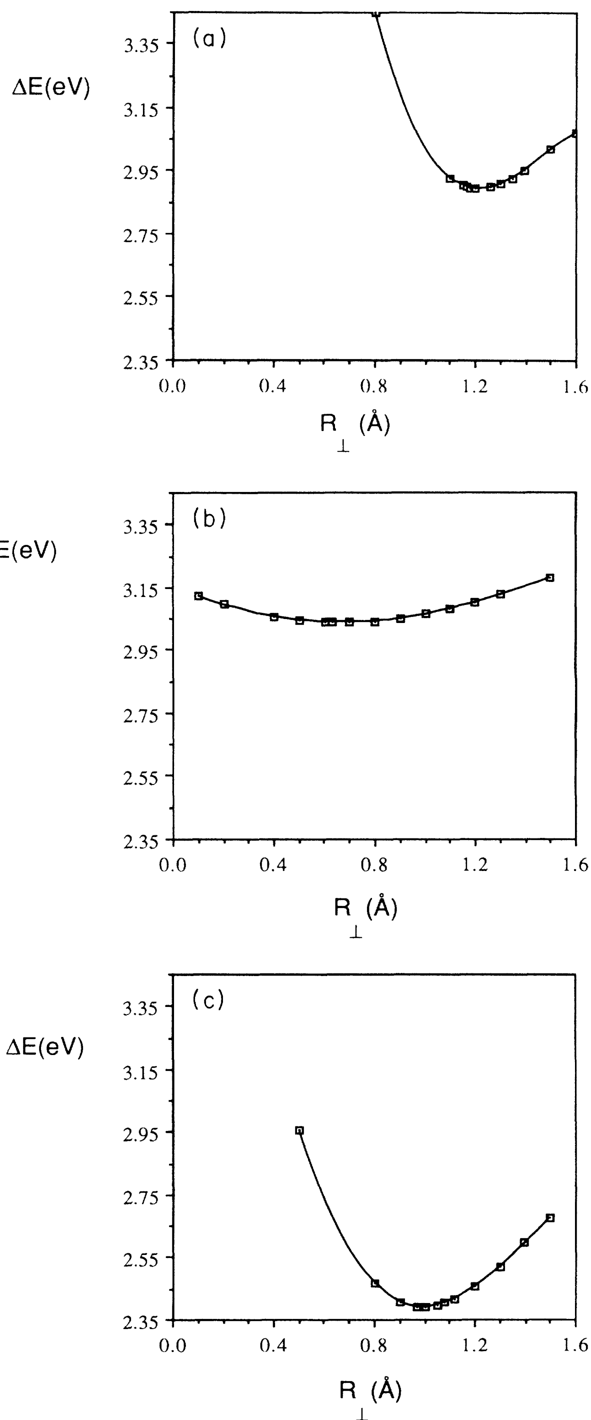

FIG. 4. GVB-CI potential-energy curves as a function of the perpendicular distance between the H and the rigid surface ($R_\perp$) for the H atom moving along the surface normal at a bridging site between dangling bonds on (a) a silicon dimer, (b) two adjacent silicon dimers in different dimer rows, and (c) two adjacent silicon dimers in the same dimer row.

sition are 1.22, 0.66, and 0.99 Å, for each of the respective H-atom diffusion pathways (see Fig. 5). Although these equilibrium perpendicular distances varied substantially from the $R_\perp$ used to obtain the curves shown in Figs. 3(a)–3(c), the difference in activation barriers by relaxing the constraint of fixed $R_\perp$ only changed the barriers by 0.1–0.2 eV. Thus, the potential-energy surface is quite flat along the surface normal direction at the transition state [see Figs. 4(a)–4(c)].

MCSCF (GVB-CI-SCF) calculations were performed at the optimized saddle-point structures ($R_{\perp,e}$ and $R_\parallel = 0$) for all three pathways. Optimization of the shapes of the orbitals in the GVB-CI wave function led to a systematic 0.1 eV decrease in the activation energy. The predicted activation barriers for the three hydrogen-diffusion pathways are listed as a function of electron correlation in Tables I, II, and III, where we see that the activation energies monotonically decrease with increasing inclusion of electron correlation. Our best level of calculation [SDT(3)+S_{val}] predicts an activation energy of 2.5 eV for a H atom hopping from one dangling bond to another on the same dimer. Since this level of CI could only be performed for the smaller case involving only one dimer, we estimated diffusion barriers for the other two cases by scaling the MCSCF values (the highest level feasible in those cases) by a factor obtained from the ratio of the SDT(3)+S_{val} energy (2.5 eV) to the MCSCF activation energy (2.8 eV) from the smaller GM-$Si_2\overline{H}_4H$ calculations. This yields predicted activation energies of 2.7 and 2.0 eV for hydrogen diffusion perpendicular to the dimer rows and along the dimer rows, respectively.

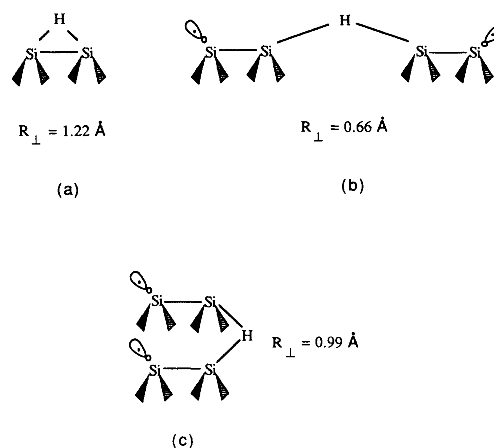

FIG. 5. Twofold bridging transition states for the three hydrogen-diffusion pathways on the Si(100)-2×1 surface. Also shown are the equilibrium distances between the H atom and Si surface plane ($R_\perp$).

Our results suggest a clear energetic trend in the hydrogen-atom surface-diffusion pathways. The barriers increase in magnitude in the following fashion: diffusion between dimers in the same row, diffusion between dangling bonds on the same dimer, and diffusion between neighboring dimers in adjacent rows. Examination of the fundamental interactions governing these processes show that the above trend coincides with intuition. For exam-

TABLE I. Equilibrium and transition-state energies for atomic H hopping from one dangling bond to another on the same Si dimer.

Calculation[a]	Total energies (hartrees) Equilibrium Si-H position	Bridging transition state	Activation energies E_{diff} (eV)[b]
GVB(2/4)-PP	−580.165 74 (4, 4)	−580.052 98 (4, 4)	3.1
GVB-RCI(2/4)	−580.165 96 (9, 17)	−580.055 26 (9, 17)	3.0
GVB-CI[c]	−580.167 95 (51, 75)	−580.061 41 (51, 75)	2.9
GVB-CI-SCF[d]	−580.168 22 (51, 75)	−580.064 47 (51, 75)	2.8
CCCI(2/4)	−580.204 00 (2785, 8373)	−580.107 21 (2785, 8373)	2.6
SDT(3)+S_{val}[e]	−580.204 96 (10 120, 27 263)	−580.112 87 (10 120, 27 263)	2.5

[a]The corresponding numbers of spatial configurations and spin eigenfunctions for each wave function are given beneath each total energy. The model cluster here is the GM-$Si_2\overline{H}_4H$ cluster, shown in Fig. 2(a). GVB-PP, RCI, and CCCI are described in Refs. 33 and 34.

[b]The diffusion activation barrier is equal to E(optimized bridging transition state) minus E(equilibrium Si-H position).

[c]Five-electron full CI within five orbitals, including one from the H atom, two from the Si-dimer bond, and two from the Si dangling-bond pair, using the GVB-PP orbitals as the CI basis.

[d]Self-consistently optimized GVB-CI wave function (see text).

TABLE II. Equilibrium and transition-state energies for atomic H hopping from one dangling bond to another on an adjacent Si dimer in an adjacent dimer row.

Calculations[a]	Total energies (hartrees) Equilibrium Si-H position	Bridging transition state	Activation energies E_{diff} (eV)[b]
GVB(4/8)-PP	−1159.702 53 (16, 16)	−1159.582 74 (16, 16)	3.3
GVB-RCI(4/8)	−1159.703 90 (81, 354)	−1159.584 47 (81, 354)	3.2
GVB-CI[c]	−1159.707 46 (3139, 8820)	−1159.595 80 (3139, 8820)	3.1
GVB-CI-SCF[d]	−1159.709 30 (3139, 8820)	−1159.599 00 (3139, 8820)	3.0
Best estimate[e]			2.7

[a]The corresponding number of spatial configurations and spin eigenfunctions for each wave function are given beneath each total energy. The model cluster here is the GM-$Si_4\overline{H}_8H$(A) cluster, shown in Fig. 2(b). GVB-PP, RCI, and CCCI are described in Refs. 33 and 34.
[b]The diffusion activation barrier is equal to E(optimized bridging transition state) minus E(equilibrium Si-H bond position).
[c]Nine-electron full CI within nine orbitals, including one from the H atom, four from the two Si-dimer bonds, and four from the two Si dangling-bonds pairs.
[d]See Table I, footnote d.
[e]The best estimate is obtained by scaling E_{diff} calculated at the GVB-CI-SCF level (3.0 eV) by a factor obtained from the ratio of the SDT(3)+S_{val} energy (2.5 eV) to the GVB-CI-SCF energy (2.8 eV) from the GM-$Si_2\overline{H}_4H$ calculations (in Table I).

ple, the barrier is highest (2.7 eV) for hopping from one dangling bond to another on a dimer in an adjacent row, primarily due to the large separation (5.24 Å) of such rows (see Fig. 1). This results in very poor orbital overlap in the bridging transition state and thus in a relatively high activation energy. Although the Si-Si bond length in the Si dimer is relatively small (2.44 Å), the orbital overlap between the two dangling bonds is poor since

TABLE III. Equilibrium and transition-state energies for atomic H hopping from one dangling bond to another on an adjacent Si dimer in the same dimer row.

Calculation[a]	Total energies (hartrees) Equilibrium Si-H position	Bridging transition state	Activation energies E_{diff} (eV)[b]
GVB(4/8)-PP	−1159.549 95 (16, 16)	−1159.456 13 (16, 16)	2.6
GVB-RCI(4/8)	−1159.551 42 (81, 354)	−1159.460 37 (81, 354)	2.5
GVB-CI[c]	−1159.559 34 (3139, 8820)	−1159.471 40 (3139, 8820)	2.4
GVB-CI-SCF[d]	−1159.562 02 (3139, 8820)	−1159.478 54 (3139, 8820)	2.3
Best estimate[c]			2.0

[a]The corresponding number of spatial configurations and spin eigenfunctions for each wave function are given beneath each total energy. The model cluster here is the GM-$Si_4\overline{H}_8H$(S) cluster shown in Fig. 2(c). GVB, RCI, and CCCI are described in Refs. 33 and 34.
[b]The diffusion activation barrier is equal to E(optimized bridging transition state) minus E(equilibrium Si-H bond position).
[c]See Table II, footnote c.
[d]See Table I, foonote d.
[e]The best estimate is obtained by scaling E_{diff} calculated at the GVB-CI-SCF level (2.3 eV) by the same factor described in footnote e, Table II.

both of these orbitals are directed away from one another [see Fig. 2(a)], resulting in a high activation energy of 2.5 eV. For diffusion within a row, however, the dangling bonds are roughly pointed in the direction of the H atom at the transition state and are separated by a moderate 3.84 Å, resulting in the best orbital overlap in the transition state and, consequently, the lowest activation energy (2.0 eV). Thus, the favorable alignment of the orbitals between dangling bonds on the same side of adjacent dimers in the same row [Fig. 2(c)] results in intrarow diffusion having the lowest barrier. This relative ordering of the three pathways leads to our major prediction concerning surface diffusion of H on Si(100)-2$\times$1: *there is a preferred direction of diffusion along the edges of dimer rows.* Note this is in contrast to theoretical studies of Si-adatom diffusion on Si(100), where although the diffusion is along dimer rows, it is predicted to occur along the middle of the rows, rather than the edges.[19,20,22] This is no doubt due to the propensity for Si to prefer multiple coordination while H prefers to be singly coordinated.

The effect of cluster size on these predictions is a concern. We therefore calculated the activation energy of a H atom hopping from one dangling bond to another on the same dimer using both the small GM-$Si_2\overline{H}_4H$ and the larger $Si_9\overline{H}_{12}H$ clusters as models. The twofold bridging transition state was explored by moving the H atom along the surface normal, while keeping it at the symmetrically bridged position. The minimum in the GVB-CI potential curve yields $R_{\perp,e}=1.28$ Å for the twofold bridging transition state on the $Si_9\overline{H}_{12}H$ cluster, 0.06 Å larger than found for the smaller GM-$Si_2\overline{H}_4H$ cluster. The GVB-CI-SCF activation energy on the $Si_9\overline{H}_{12}H$ cluster is predicted to be 2.5 eV, which is 0.3 eV lower than the same level of calculation on the smaller GM-$Si_2\overline{H}_4H$ cluster (2.8 eV). Thus, the estimated cluster-size effect on the activation energetics is $\sim$0.3 eV, which is still smaller than the difference in predicted activation energies for diffusion parallel versus perpendicular to dimer rows. Thus, our qualitative conclusions are expected to hold up for more exact descriptions of the surface (i.e., larger clusters).

Regarding the impact of this effect on our current best estimates for the diffusion activation barriers, unfortunately we cannot carry out similar calculations to estimate the cluster-size effect for the other diffusion pathways because of the increased computational complexity engendered by an even larger cluster requirement (since two Si dimers are involved). Therefore, we cannot say, for example, that all of our best estimates from the smaller cluster calculations will be reduced by 0.3 eV, since we do not know the cluster-size effect for different clusters and for different levels of electron correlation. Thus, it would be misleading to suggest that all barriers will drop by an additional 0.3 eV if large enough clusters were used. We therefore stand by our estimates given in Tables I–III.

The predicted difference of 0.7 eV in the activation energies for hydrogen diffusion along and perpendicular to the surface dimer rows suggests that migration should be strongly anisotropic, consisting of one-dimensional hydrogen diffusion on an individual terrace of the Si(100)-2$\times$1 surface. However, since most steps on the Si(100) surface are one atom high, this results in an equivalent number of dimers oriented at 90° to the dimers on the adjacent terrace. Thus anisotropic diffusion will not be observed on surfaces with single-atom steps. If a surface is cut to allow double-atom steps to form, then this vicinal surface will have all the dimer rows aligned on all terraces so that anisotropic diffusion should in principle be measurable via, e.g., anisotropic hole burning followed by LITD measurements.[37] Finally, as our current best estimate for the diffusion activation barrier of 2.0 eV is within the reported range (2.0–3.0 eV) of activation energies for H_2 β_1 desorption, it may be that diffusion is the rate-limiting step in desorption of H_2. Certainly, it is clear that at temperatures where H_2 is desorbing from silicon, H atoms are also diffusing along the dimer rows. Investigations of possible desorption pathways will be published elsewhere.[38]

ACKNOWLEDGMENTS

This work was supported by the Air Force Office of Scientific Research (Grant No. AFOSR-89-0108). One of us (E.A.C.) also acknowledges the National Science Foundation and the Camille and Henry Dreyfus Foundation for partial support of this work. The other (C.J.W.) is grateful for partial support by the Products Research Corporation.

[1] M. Jasinski and S. M. Gates, Acc. Chem. Res. **24**, 9 (1991).
[2] H. Ibach, H. Wagner, and D. Bruchmann, Solid State Commun. **42**, 457 (1982).
[3] L. Kubler, E. K. Hlil, D. Bolmont, and G. Gewinner, Surf. Sci. **183**, 503 (1987).
[4] R. J. Hamers, Ph. Avouris, and F. Bozso, Phys. Rev. Lett. **59**, 2071 (1987).
[5] P. Nachtigall, K. D. Jordan, and K. C. Janda, J. Chem. Phys. **95**, 8652 (1991).
[6] C. J. Wu and E. A. Carter, Chem. Phys. Lett. **185**, 172 (1991).
[7] K. Sinniah, M. G. Sherman, L. B. Lewis, W. H. Weinberg, J. T. Yates, Jr., and K. C. Janda, Phys. Rev. Lett. **62**, 567 (1989).
[8] K. Sinniah, M. G. Sherman, L. B. Lewis, W. H. Weinberg, J. T. Yates, Jr., and K. C. Janda, J. Chem. Phys. **92**, 5700 (1990).
[9] M. L. Wise, B. G. Koehler, P. Gupta, P. A. Coon, and S. M. George, Surf. Sci. **258**, 166 (1991).
[10] U. Höfer, L. Li, and T. F. Heinz, Phys. Rev. B **45**, 9485 (1992).
[11] B. G. Koehler, C. H. Mak, D. A. Arthur, P. A. Coon, and S. M. George, J. Chem. Phys. **89**, 1709 (1988).
[12] G. A. Reider, U. Höfer, and T. F. Heinz, Phys. Rev. Lett. **66**, 1994 (1991).
[13] B. M. Rice, L. M. Raff, and D. L. Thompson, J. Chem. Phys. **88**, 7221 (1988).
[14] G. Ehrlich and K. Stolt, Ann. Rev. Phys. Chem. **31**, 603 (1980).
[15] C. H. Mak, J. L. Brand, A. A. Deckert, and S. M. George, J. Chem. Phys. **85**, 1676 (1986).
[16] C. H. Mak, J. L. Brand, B. G. Koehler, and S. M. George,

Surf. Sci. **188**, 312 (1987).
[17]C. H. Mak, J. L. Brand, B. G. Koehler, and S. M. George, Surf. Sci. **191**, 108 (1987).
[18]P. Feulner and D. Menzel, Surf. Sci. **154**, 465 (1985).
[19]G. Brocks, P. J. Kelly, and R. Car, Phys. Rev. Lett. **66**, 1729 (1991).
[20]Z. Y. Zhang, Y.-T. Lu, and H. Metiu, Surf. Sci. **248**, L250 (1991).
[21]D. Srivastava, B. J. Garrison, and D. W. Brenner, Phys. Rev. Lett. **63**, 302 (1989).
[22]D. Srivastava and B. J. Garrison, J. Chem. Phys. **95**, 6885 (1991).
[23]C. J. Wu and E. A. Carter, J. Am. Chem. Soc. **113**, 9061 (1991).
[24]C. J. Wu and E. A. Carter, Phys. Rev. B **45**, 9065 (1992).
[25]A. Redondo, W. A. Goddard III, C. A. Swarts, and T. C. McGill, J. Vac. Sci. Technol. **19**, 498 (1981).
[26]A. Redondo and W. A. Goddard III, J. Vac. Sci. Technol. **21**, 344 (1982).
[27]A. K. Rappé, T. A. Smedley, and W. A. Goddard III, J. Phys. Chem. **85**, 1662 (1981).
[28]T. H. Dunning, Jr., J. Chem. Phys. **53**, 2823 (1970).
[29]S. Huzinaga, J. Chem. Phys. **42**, 1293 (1965).
[30]F. W. Bobrowicz and W. A. Goddard III, *Methods of Electronic Structure Theory* (Plenum, New York, 1977), Vol. 3, pp. 79–127.
[31]H. B. Schlegel, J. Comput. Chem. **3**, 214 (1982).
[32]M. Dupuis and H. F. King, J. Chem. Phys. **68**, 3998 (1978).
[33]E. A. Carter and W. A. Goddard III, J. Chem. Phys. **88**, 3132 (1988).
[34]E. A. Carter and W. A. Goddard III, J. Chem. Phys. **88**, 1752 (1988).
[35]C. J. Wu and E. A. Carter, J. Am. Chem. Soc. **112**, 5893 (1990).
[36]C. J. Wu and E. A. Carter, J. Phys. Chem. **95**, 8352 (1991).
[37]M. V. Arena, E. D. Westre, and S. M. George, J. Chem. Phys. **96**, 808 (1992).
[38]C. J. Wu and E. A. Carter (unpublished).